Supporting Information: Tunable lattice thermal conductivity of twisted bilayer MoS_2

Soham Mandal[1], Indrajit Maity[1,2], Anindya Das[3], Manish Jain[4], and Prabal K. Maiti[*5]

[1,3,4,5]Centre for Condensed Matter Theory, Department of Physics, Indian Institute of Science, Bangalore-560012, India
[2]Department of Materials, Imperial College London, South Kensington Campus, London SW7 2BX, UK

MD Simulation

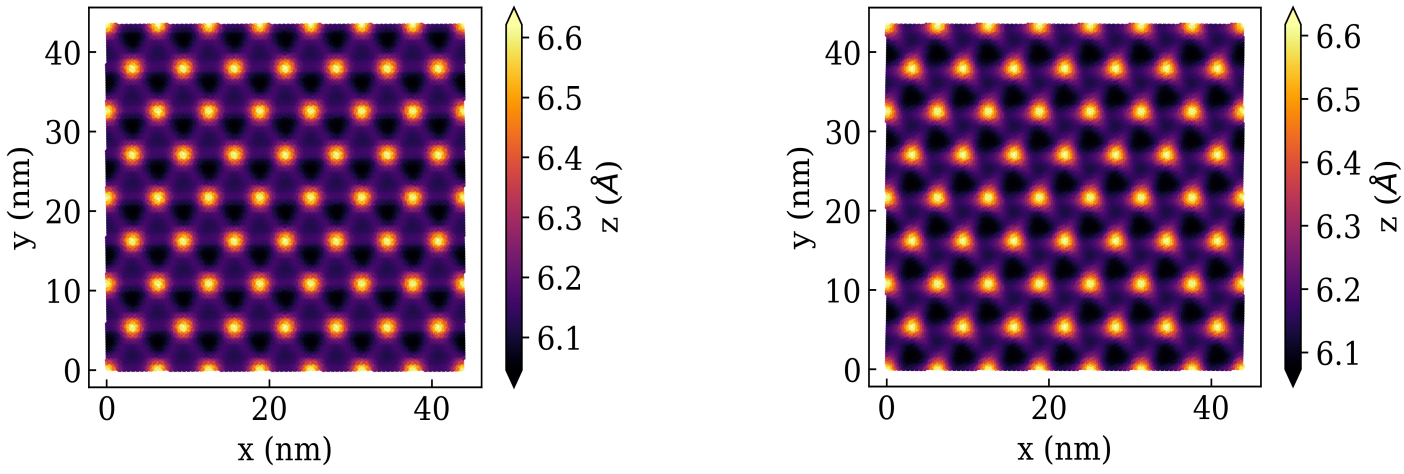

Figure 1: Heat map of interlayer separation landscape of (a) 2.87° and (b)57.13° twisted system after structural relaxation.Relaxation of the system is done with potential energy tolerance of 10^{-12} and force tolerance of $10^{-10} eV/\mathring{A}$. The ILS is higher in AA stacking region where two atoms of the bilayer system exactly on top of each other and also varies periodically with moiré pattern as reported in literature[1]. Lattice reconstruction of tBL-MoS_2 close to angle 60° was reported recently[2].

Once the system has reached in a steady state after thermal equilibration run and 500 ps of NEMD the temperature of each slab along the heat flux direction is recorded for 100 ps. The average of the temperature distribution for the last 100 ps is shown in figure 2(a) for 200 nm long 21.78° twisted bilayer system. The width of the system is 14.43 nm (241×10 moiré unitcell). Temperature distribution in the region close to heating and cooling is non-linear. This happens due to rapid change of the kinetic energy and the region does not get time to reach equilibrium. Once a steady temperature gradient is generated the slope along heat flux direction excluding the nonlinear region is found. κ is then computed from the Fourier law of heat transport $\mathbf{J} = -\kappa A \nabla T$. Here $\mathbf{J}$ is half of J_x as heat flux divides into two direction uniformly from heat bath region at the center. J_x is calculated from the slope if cumulative kinetic energy exchange between heating and cooling region as shown in figure 2(b).

*Email: maiti@iisc.ac.in

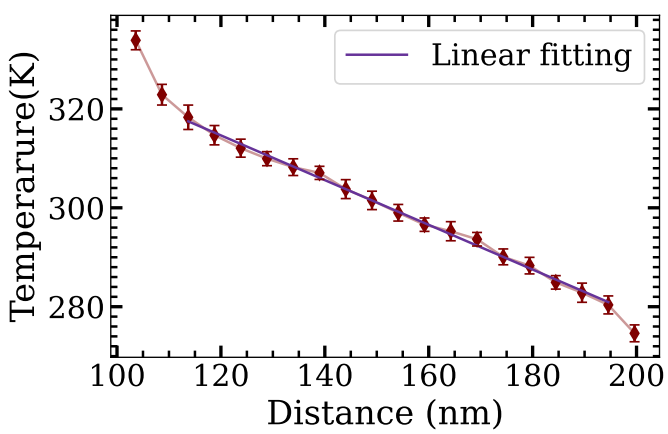

(a)

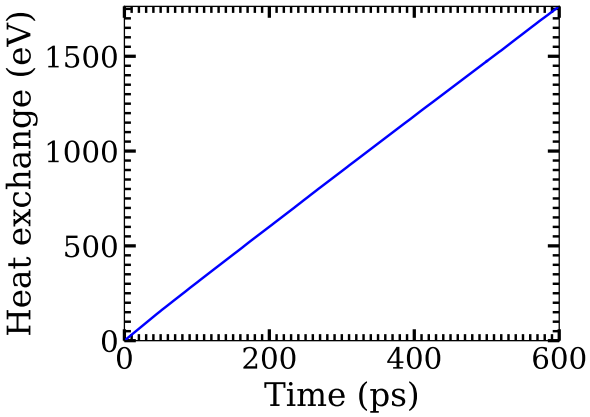

(b)

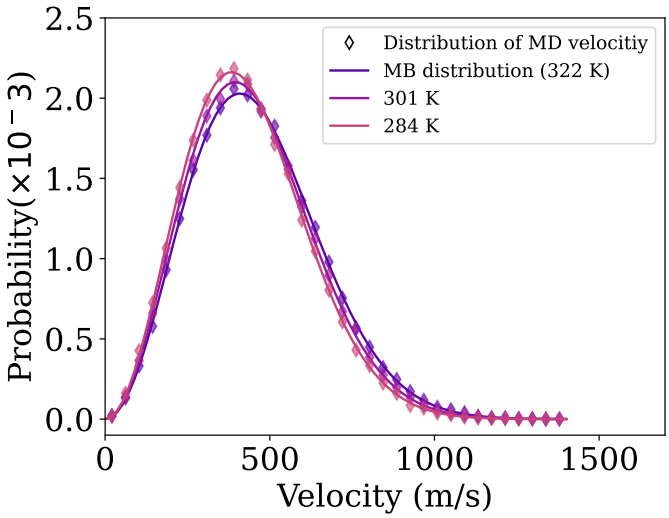

(c)

Figure 2: (a) Temperature profile of one half of a 200 nm long 21.78° twisted system after NEMD simulation. The non-linear region close to heat-bath and heat-sink region is excluded from calculation of the slope. (b) Accumulated energy at heat bath region due to kinetic energy exchange of Müller-Plathe algorithm. Heat flux is calculated from slope of the cumulative energy vs. time plot. (c) Fitting of Maxwell-Boltzmann velocity distribution for each of the constant temperature strip along the heatflux direction after the system reached in a steady state. At steady-state of NEMD each constant temperature strip locally achieve a equilibrium state.

First principles computation

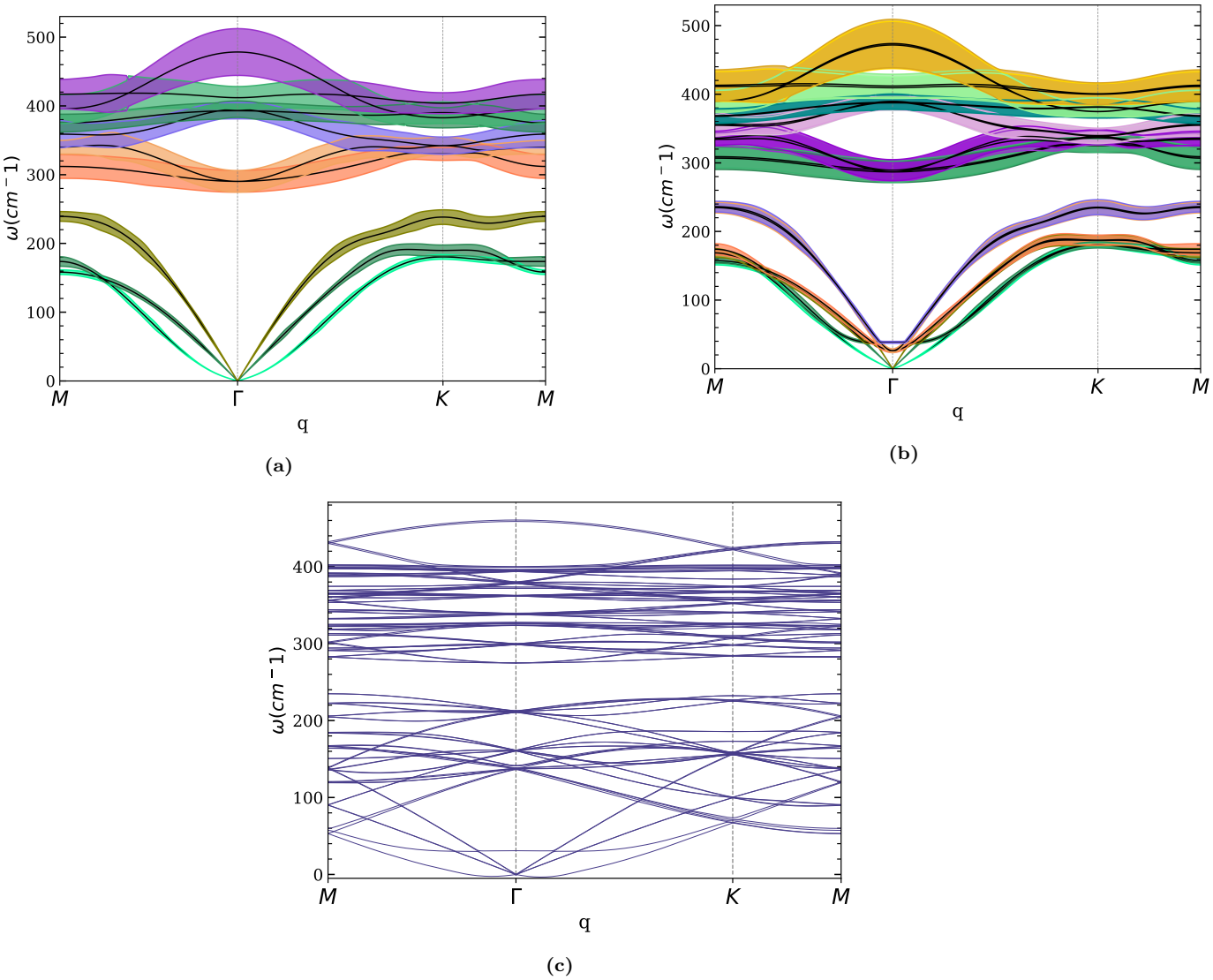

Figure 3: Phonon dispersion of (a)single layer and (b)bilayer MoS_2. The anharmonic phonon broadening is represented with filled color along the both side of each phonon band. The widening due to anharmonic scattering is expressed in cm^{-1} and magnified by a factor 50. (c) Phonon dispersion of 21.78° twisted bilayer MoS_2.

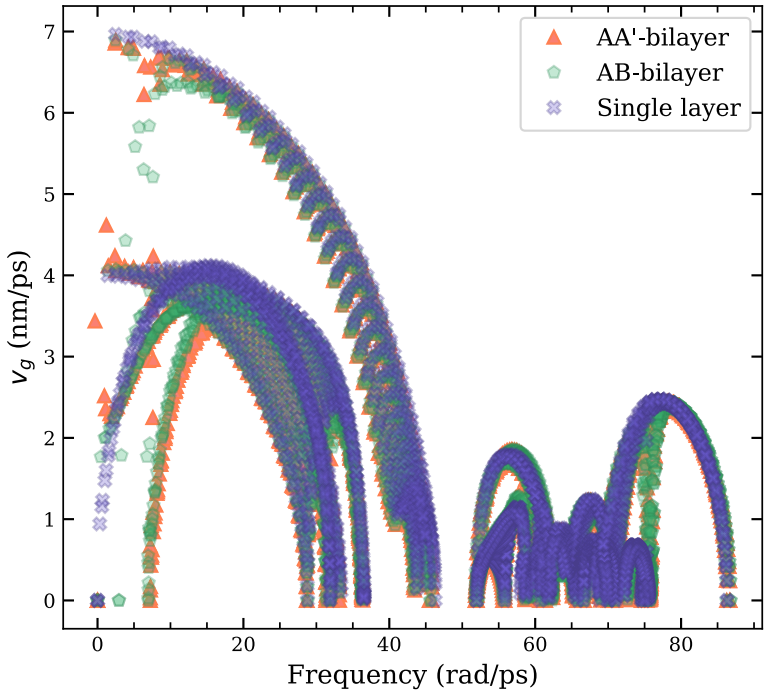

Figure 4: Phonon group velocity for all the phonon modes in first BZ. v_g is similar for single layer and two different stacking of bilayer. This indicates that phonon group velocity does not influence the thermal conduction. Phonon scattering rate is the dominating physical phenomena behind the change of thermal transport coefficient.

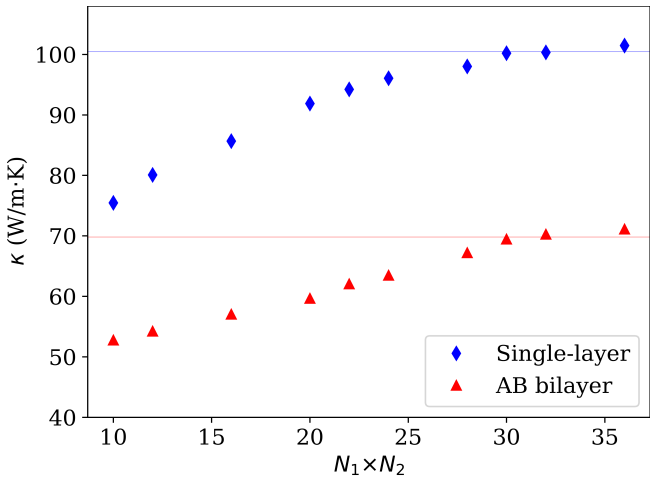

(a)

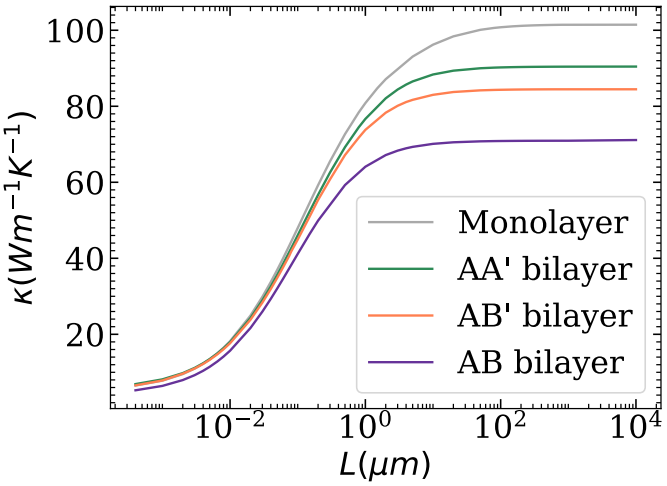

(b)

Figure 5: (a) Convergence of κ with q-grid points along the axis. (b) Convergence of κ with the sample size of monolayer and bilayer is summarized in the figure.The κ depends on sample size or nanowire diameter[3](L) due to boundary scattering which limits the intrinsic value of thermal conductivity in materials. If system dimension is smaller than the effective mean free path (Ł$_{eff}$) [4] [5]of the collective excitation of phonon, measured thermal conductivity may scale down from its intrinsic value. For Fourier law to be applied in heat conduction the distance between heat source and sink needs to be few L_{eff} long. The L_{eff} of single layer-MoS_2 at 300K is near 55 μm. κ converges in further increasing L as shown in figure and the system dimension is said to reach in a diffusive regime. The diffusive limit of $AA^{'}$ and $AB^{'}$ stacked bilayer is found about 10 μm and for AB bilayer near 6 μm. Intrinsic thermal conductivity for $AA^{'}$, $AB^{'}$ and AB stacking of bilayer is found 90.44, 84.47 and 71.11 $W/m \cdot K$ respectively at 300K.The L_{eff} decreases from single layer to bilayer and further decreases in 3-D system was reported for graphene and graphite [5]. The experimental evidence of size dependence of thermal conductivity for suspended monolayer and bilayer TMDCs is also reported recently[6].

References

[1] Mit H. Naik et al. "Kolmogorov–Crespi Potential For Multilayer Transition-Metal Dichalcogenides: Capturing Structural Transformations in Moiré Superlattices". *The Journal of Physical Chemistry C* 123.15 (2019), pp. 9770–9778.

[2] Indrajit Maity et al. "Reconstruction of moiré lattices in twisted transition metal dichalcogenide bilayers". *Phys. Rev. B* 103 (12 Mar. 2021), p. L121102.

[3] Wu Li et al. "Thermal conductivity of diamond nanowires from first principles". *Phys. Rev. B* 85 (19 May 2012), p. 195436.

[4] M. Asen-Palmer et al. "Thermal conductivity of germanium crystals with different isotopic compositions". *Phys. Rev. B* 56 (15 Oct. 1997), pp. 9431–9447.

[5] Giorgia Fugallo et al. "Thermal Conductivity of Graphene and Graphite: Collective Excitations and Mean Free Paths". *Nano Letters* 14.11 (Nov. 2014), pp. 6109–6114.

[6] Yifei Yu et al. "In-Plane and Interfacial Thermal Conduction of Two-Dimensional Transition-Metal Dichalcogenides". *Phys. Rev. Applied* 13 (3 Mar. 2020), p. 034059.